COMPOSITE DESIGN AND MANUFACTURING

Composite Design and Manufacturing, 2025, **1(2)**, 69–76
https://doi.org/10.1093/cdm/wqaf007
Research Article

Towards strength–ductility balance in a Ti-6Al-4V alloy through microstructure optimization by composite hot forging and two-step annealing processes

Shenshi Jiang[1], Guangqing Zhang[1], Lisong Zhu[1], Qian Wang[1], Feijun Qu[1], Jun Wang[2], Yao Lu[2], Jian Han[1,*]

[1]School of Mechanical, Materials, Mechatronic and Biomedical Engineering, University of Wollongong, Wollongong, Northfields Ave, NSW 2522, Australia
[2]Welding and Additive Manufacturing Centre, Cranfield University, College Road, Bedfordshire MK430AL, United Kingdom

*Corresponding author. School of Mechanical, Materials, Mechatronic and Biomedical Engineering, University of Wollongong, Wollongong, Northfields Ave, NSW 2522, Australia. E-mail: jianh@uow.edu.au.

Abstract

Objectives: Obtaining strength–ductility balance in titanium alloys remains a challenge to this day. In this work, we improve the strength–ductility synergy of a Ti-6Al-4V alloy through specialized hot forging and two-step annealing processes.

Methods: During hot forging, the large equiaxed grains undergo minimal change, while all the lamellar α grains spheroidize to fine equiaxed grains due to severe dynamic recrystallization. During subsequent annealing and water quenching, the large equiaxed grains remain unchanged, and the martensite transformation occurs within fine equiaxed grains, leading to the microstructures composed of large equiaxed grains and nanosized acicular α′ martensite grains in the water quenched (WQ) alloy.

Results and conclusion: Compared to the hot forged (FG) alloy, the WQ alloy exhibited a significantly increased tensile strength and a decreased elongation. The strengthening effect came from the high dislocation density, high-density grain boundaries, and dense twin boundaries in the region of α′ martensite. The short-time annealed (ST) alloy after the second-step short-time annealing then showed a similar grain size and morphology to the WQ alloy. However, the dislocation density in large equiaxed grains dramatically decreased. This caused an increased elongation without sacrificing strength compared with the WQ alloy, implying the superior strength–ductility balance.

Keywords: titanium alloy; cold-stretching; α+α′ nanostructure; α′ nano twins; strength–ductility synergy

1. Introduction

Titanium alloys are indispensable structural materials for advanced engineering applications owing to their excellent specific strength, corrosion resistance and biocompatibility, especially in fields of aerospace components, biomedical implants and marine heat exchangers [1, 2]. Strength and plasticity are generally at odds with each other in materials science, so the trade-off between strength and plasticity in the design of advanced titanium alloys remains a thorny scientific issue [3–6].

The microstructure of titanium alloys varies according to the manufacturing method, heat treatment, and chemical composition of the alloy, and different microstructures directly affect their mechanical properties [7, 8]. Hua *et al.* [9] obtained a full fine isometric microstructure with an average size of 160 nm by optimizing the heat treatment of a metastable β titanium alloy (Ti-5Al-5Mo-5V-3Cr-0.5Fe) with multiple isothermal compression and stress relaxation, which increased the yield strength of the titanium alloy. Dumas *et al.* [10] proposed that the coupling of pulsed current and hydrogen can cause the evolution of the lamellar microstructure in the as-cast Ti-6Al-4V alloy into the globular or needle-like microstructure, and the mechanical properties were significantly improved. Ouyang *et al.* [11] used laser shock peening (LSP) technique to optimize the microstructure near the surface of hot-forged Ti-6Al-4V alloys, reconstructing the ultrafine and coarse crystals to form a gradient grain structure from the surface to the interior. The alloy with three-time LSP has achieved the highest microhardness, wear resistance and tensile properties. In addition, Lett *et al.* [12] performed heat treatments with different annealing temperatures (575–1050°C) and cooling conditions on the cold sprayed Ti-6Al-4V samples to improve the low tensile properties of the deposited material. Annealing at temperatures in the 950 to 1050°C range was efficient to obtain high strength and ductility combinations. Shen *et al.* [13] investigated the effects of annealing temperatures from 450°C to 800°C on the microstructure and mechanical properties of a new α + β titanium alloy designed, Ti-6Al-4V-2Mo-2Fe (Ti6422), and obtained ultra-high strengths (1340 MPa, 1390 MPa) and good plasticity (11.8%) at annealing temperatures of 500°C and 550°C.

The design of heterogeneous structure materials has been demonstrated to be an effective way to achieve synchronized strength–ductility of materials [14, 15]. The large differences in mechanical properties lead to significant heterogeneous deformation-induced (HDI) strengthening and back-stress

Received: 11 August 2025; **Revised:** 28 August 2025; **Accepted:** 3 September 2025
© The Author(s) 2025. Published by Oxford University Press on behalf of Taiyuan University of Technology.
This is an Open Access article distributed under the terms of the Creative Commons Attribution License (https://creativecommons.org/licenses/by/4.0/), which permits unrestricted reuse, distribution, and reproduction in any medium, provided the original work is properly cited.

hardening, resulting in a dual effect of strengthening and toughening [16–18]. Lin *et al.* [19] prepared a heterogeneous structure (HS) with an alternating distribution of coarse and fine α lamella in bimodal Ti6242 alloy by fast heat treatment. The enhanced strength and plasticity are attributed to HDI strengthening and coordinated deformation of HS, respectively. Jia *et al.* [20] fabricated a highly HS with micron-sized primary α and nanoscale secondary α precipitates was fabricated by activating the ω-assisted α nucleation transformation pathway that operates in metastable β titanium alloys alone, leading to an enhanced mechanical property. In addition, Meng *et al.* [21] designed a HS in Ti-6Al-4V alloy via cryogenic pre-stretching at liquid nitrogen temperature. This process simultaneously achieved an increase in the strength of the material and the maintenance of its ductility. Yang *et al.* [22] obtained a β HS with heterogeneous grain size and defects in Ti-7Mo-3Nb-3Cr-3Al metastable β titanium alloy by hot rolling and partial recrystallization. The yield strength at room temperature was 1360 MPa, the tensile strength was 1430 MPa, and the elongation was 8.1%. Similarly, Feng *et al.* [23] designed to obtain a metastable β titanium alloy of HS consisting of deformed and recrystallized grains by simple cold rolling and short-term annealing, and the combined effect of HDI hardening and phase transition-induced plasticity (TRIP) effect resulted in a simultaneous increase in yield strength and plasticity of the alloy. Dai *et al.* [24] prepared the α + β Ti-5Al-7.5V-0.5Mo-0.5Zr-0.5Si (TC5751S) alloy containing silicide. The mechanical properties of the alloys were enhanced with the increased precipitation of nanoscale secondary α precipitates, as well as the precipitation of microscale primary α and (Ti, Zr)5Si3 silicide, verifying the compensatory mechanism between the silicide and the heterogeneous α phase.

Although the heterostructured titanium alloys have been widely reported to exhibit enhanced high strength and high ductility. However, most previous reports only concentrated on single type heterostructure, such as grain size gradient structure and phase gradient structure. It is valuable to further explore and design new multi-scale heterostructures. In this study, we improve the strength–ductility synergy of a Ti-6Al-4V alloy through specialized hot forging and two-step annealing processes. The processed alloy shows the microstructure composed of large equiaxed grains and nanosized acicular α′ martensite grains. The formation mechanism of such unique dual-phase α + α′ structure was revealed by various characterization techniques. The mechanisms of strengthening and ductility improvement were discussed in detail.

2. Experimental methods

2.1 Thermal-mechanical processing

A bimodal structured Ti-6Al-4V alloy bar (T_β = 990°C) was used in this work. The larger equiaxed and lamellar α grains coexist in the alloy. The thermal-mechanical processing of Ti-6Al-4V alloy in this work contains hot forging and two-step annealing processes (Fig. 1). First, the cylindrical Ti-6Al-4V alloy (diameter: 40 mm; height: 60 mm) was heated to 920°C (α + β region) and stayed at this temperature for 10 mins to reach a homogeneous temperature distribution. Then, the specimens were compressed by 60% at 920°C at a strain rate of 0.01/s. The hot forging process was performed using an UTM4304 electronic universal testing machine equipped with a heating furnace. After hot forging, the specimen was air cooled to room temperature. The hot forged specimen is hereafter referred to as "FG". Then, the specimen was heated to 950°C and annealed at this temperature for 10 minutes, followed by water quenching. The water quenched specimen is hereafter referred to as "WQ". Finally, the specimen was heated to 380°C and annealed at this temperature for 5 minutes, followed by air cooling, which is hereafter referred to as "ST".

2.2 Microstructural characterization

The FG, WQ, and ST specimens were cut for subsequent microstructural characterization. The normal plane of the specimen (parallel to the forging direction) was metallographically polished by polishing papers and SiO_2 solution. To improve the surface quality, the specimen was then electropolished in a solution of 10% perchloric acid and 90% ethanol for 50 s at 30 V. The microstructural characterization was performed using an electron-backscatter diffraction detector (EBSD, Oxford Nordlys Max3) equipped on a scanning electron microscope (SEM, JSM-7800F) operated at 20 kV. To better reveal the microstructural features, the foil specimens were prepared by ion beam milling and then characterized by transmission electron microscope (TEM, FEI Talos F200X G2).

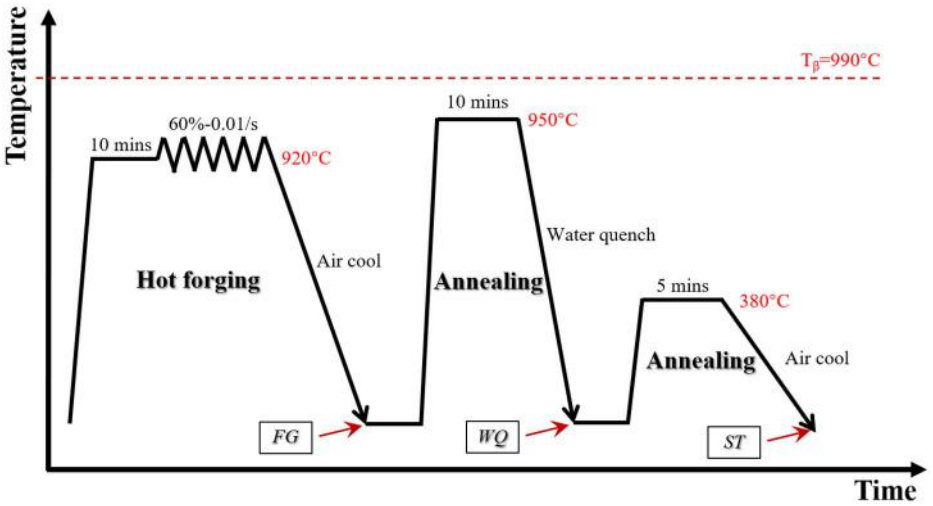


Figure 1. Schematic diagram of three thermal-mechanical processing routes.

2.3 Tensile test

The FG, WQ, and ST specimens were cut for tensile tests. The gauge dimensions of tensile specimens are 6 mm in width, 2 mm in thickness, and 12 mm in length. The tensile tests were conducted at the strain rate of 0.001/s using an Instron 5982 testing machine.

3. Results

3.1 Microstructure evolution during hot forging and two-step annealing processes

The EBSD orientation maps of FG, WQ, and ST alloys were displayed in Fig. 2. For FG alloy, the large equiaxed and small equiaxed grains can be clearly observed in Fig. 2a. The large equiaxed grains were inherited from the as-received alloy, implying that the large equiaxed grains hardly changed during hot forging. However, the deformation at high temperature caused the dynamic recrystallization of lamellar α grains, so that almost all the lamellar α grains have recrystallized to fine equiaxed grains. Besides, the WQ alloy shows a heterostructure composed of the large equiaxed grains and fine acicular grains. The formation of such microstructure indicates the occurrence of martensite transformation during water quenching. Specifically, all the fine equiaxed grains transformed to α′ martensite and the large equiaxed grains remained unchanged in the WQ alloy. Notably, the ST alloy exhibits similar microstructure to the WQ alloy, which both have large equiaxed grains and fine acicular α′ martensite grains. This is because the second-step annealing temperature is low and the time is short, so that the decomposition of α′ martensite hardly occurs. Figure 2d–f show the inverse pole figures (IPF) of the FG, WQ, and ST alloys. The FG alloy shows a (0001) texture with an intensity of 2.06 MUD. After subsequent first-step annealing and water quenching, the (0001) texture intensity significant decreases in the WQ alloy. This may be attributed to the martensite transformation during water quenching, in which the various orientated martensite forms and weakens the texture. For the ST alloy, the texture intensity is extremely weak and the (0001) texture almost disappears, indicating the homogeneous grain orientation distribution.

The grain boundary maps of FG, WQ, and ST alloys were displayed in Fig. 3. For FG alloy, large amounts of low angle grain boundaries (LAGBs) exist (34.2%), which dominantly distribute

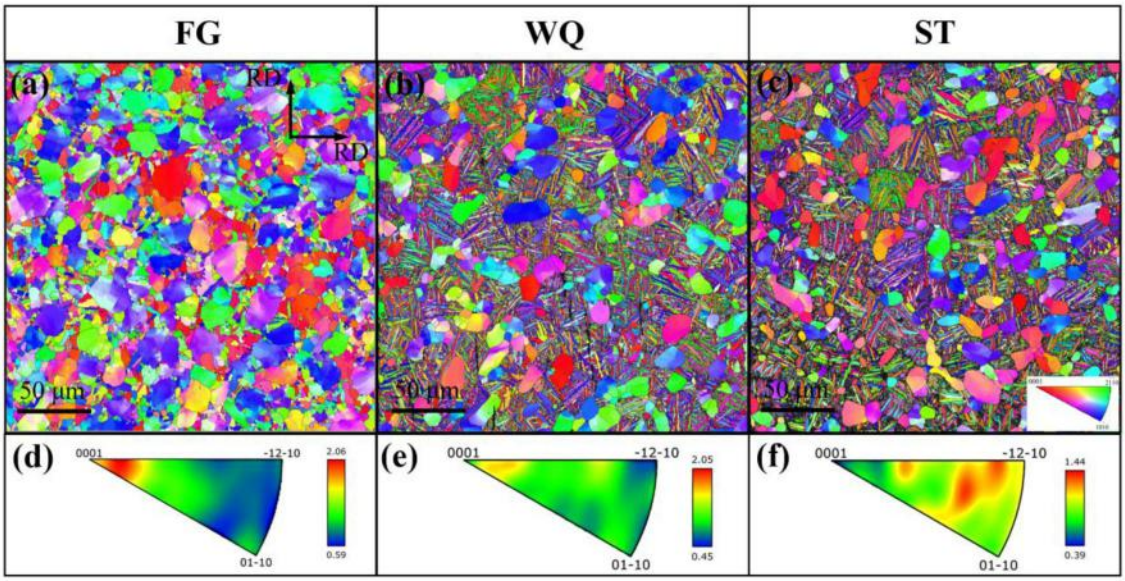


Figure 2. (a–c) EBSD orientation maps of the FG, WQ, and ST alloys, respectively. RD in the figure represents the radial direction, which is perpendicular to the forging direction of the alloy. It is noted that the tensile direction during tensile tests is parallel to the RD. (d–f) IPFs (referenced to RD) of the FG, WQ, and ST alloys, respectively.

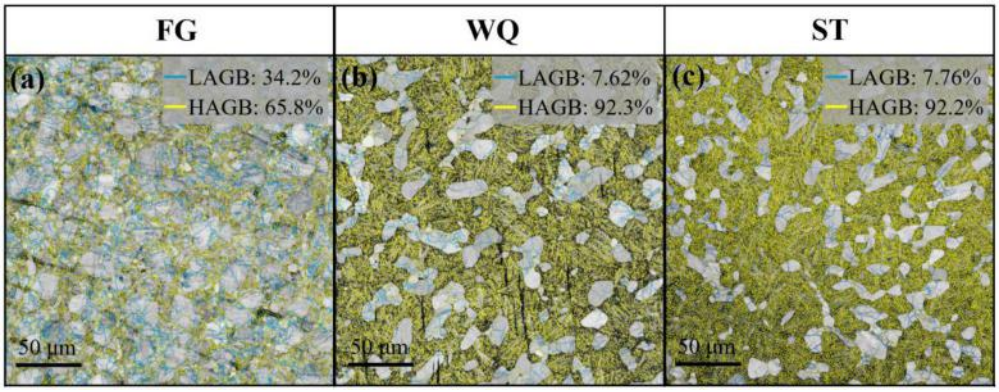


Figure 3. (a–c) Grain boundary maps of the FG, WQ, and ST alloys, respectively. The fraction of HAGB and LAGB are shown in the figures.

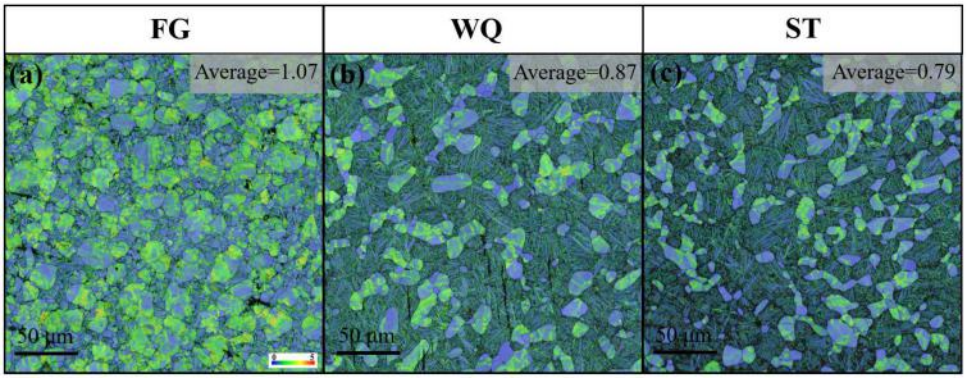


Figure 4. (a–c) KAM maps of the FG, WQ, and ST alloys, respectively. The average KAM values are shown in the figures.

within the large equiaxed grains. This implies that the hot forging promotes the subgrain formation within the large equiaxed grains. The high angle grain boundaries (HAGBs) locate among fine recrystallized equiaxed grains, indicating the complete recrystallization. In this work, the hot deformation degree is not enough for the complete recrystallization of large equiaxed grains, so that the recrystallization only occurs in the lamellar grains. For the WQ and ST alloys, the fraction of LAGB significantly decreases and the fraction of HAGB significantly increases. This is because the α′ martensite grains have extremely small size, which provide large amounts of HAGBs.

The Kernel Average Misorientation (KAM) maps of FG, WQ, and ST alloys were displayed in Fig. 4. KAM angle is a measure of local grain misorientation, which refers to the average misorientation between an EBSD pixel and its neighboring pixels. The KAM value reflects the local misorientation and can be used to evaluate the density of geometrically necessary dislocation (GND). For FG alloy, the average KAM value is the largest (1.07) among these three alloys. This is because the hot deformation may induce the defects to the alloy, which dominantly locates around the LAGBs and HAGBs. For the WQ and ST alloys, the average KAM value decreases owing to the first-step and second-step annealing processes. The accumulated dislocations in the FG alloy strongly annihilate during hot annealing. However, the martensite transformation is known to induce the internal stress and defects. Therefore, the total dislocation densities in the WQ and ST alloys are lower than that of the FG alloy, but the difference is not significant. Moreover, the dislocation density in the ST alloy (0.79) is lower than that of the WQ alloy (0.87). This is because the second-step annealing process can further release the dislocation accumulation at a certain degree.

3.2 Tensile mechanical properties

Figure 5 displays the engineering stress-strain curves of the FG, WQ, and ST specimens. The FG specimen has a tensile strength of 921 MPa and an elongation of 12.6%. After subsequent annealing and water quenching, the WQ alloy shows an enhanced tensile strength of 1124 MPa and a decreased elongation of 10.81%. After second-step annealing and air quenching, the ST alloy shows an increased elongation (12.3%) and maintains a similar high tensile strength (1132 MPa) compared to the WQ alloy, implying the superior strength–ductility balance. Notably, compared to the FG alloy, the ST alloy shows a significant increase of tensile strength without sacrificing the ductility. This indicates that the composite hot forging and two-step annealing processes in this work are available and effective to achieve outstanding mechanical properties in titanium alloys.

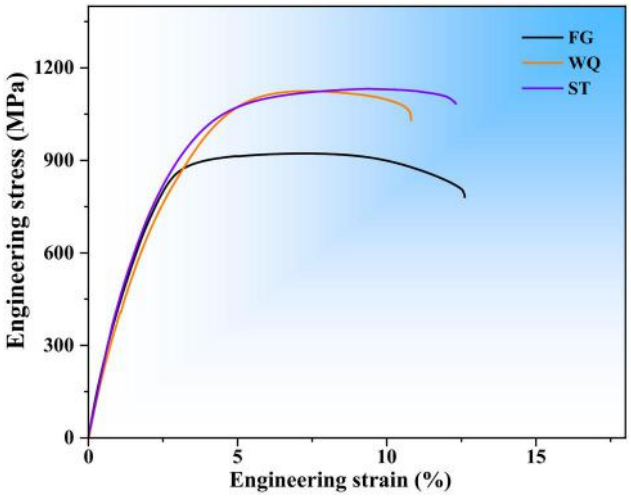


Figure 5. Engineering stress–strain curves of the FG, WQ, and ST alloys.

4. Discussion

4.1 Strengthening mechanism of the WQ alloy with dual phase structure

It was widely reported that two kinds of martensite phases may exist in titanium alloys, *hcp* α′ martensite and orthorhombic α″ martensite. Generally, the acicular α′ phase is strong and hard, which can increase the strength of the alloy but decrease the ductility [25–27]. In the present work, the WQ alloy exhibits a microstructure composed of large equiaxed α grains and acicular α′ martensite grains. The tensile strength of the WQ alloy is obviously higher than that of the FG alloy. The strengthening mechanism of the WQ alloy with dual phase structure can be explained by the TEM results shown in Fig. 6.

Figure 6a clearly shows the dual phase structure in the WQ alloy, in which the large equiaxed α grains and acicular α′ martensite grains can be identified. It's noted that the elemental distribution is homogeneous between large equiaxed α grains and acicular α′ martensite grains, which is confirmed by the EDS maps in Fig. 6c1-c4. Figure 6d–f displays the microstructural features of the large equiaxed α grain. The subgrains appear in some of the equiaxed α grains, which agrees to the aforementioned EBSD results. Besides, in some of the equiaxed α grains, the high-density dislocations and dislocation tangle can be observed (Fig. 6d). However, in most of the large equiaxed α grains, the dislocation lines arrange parallelly without accumulation (Fig. 6b and f). Such dislocation distribution can be attributed to the

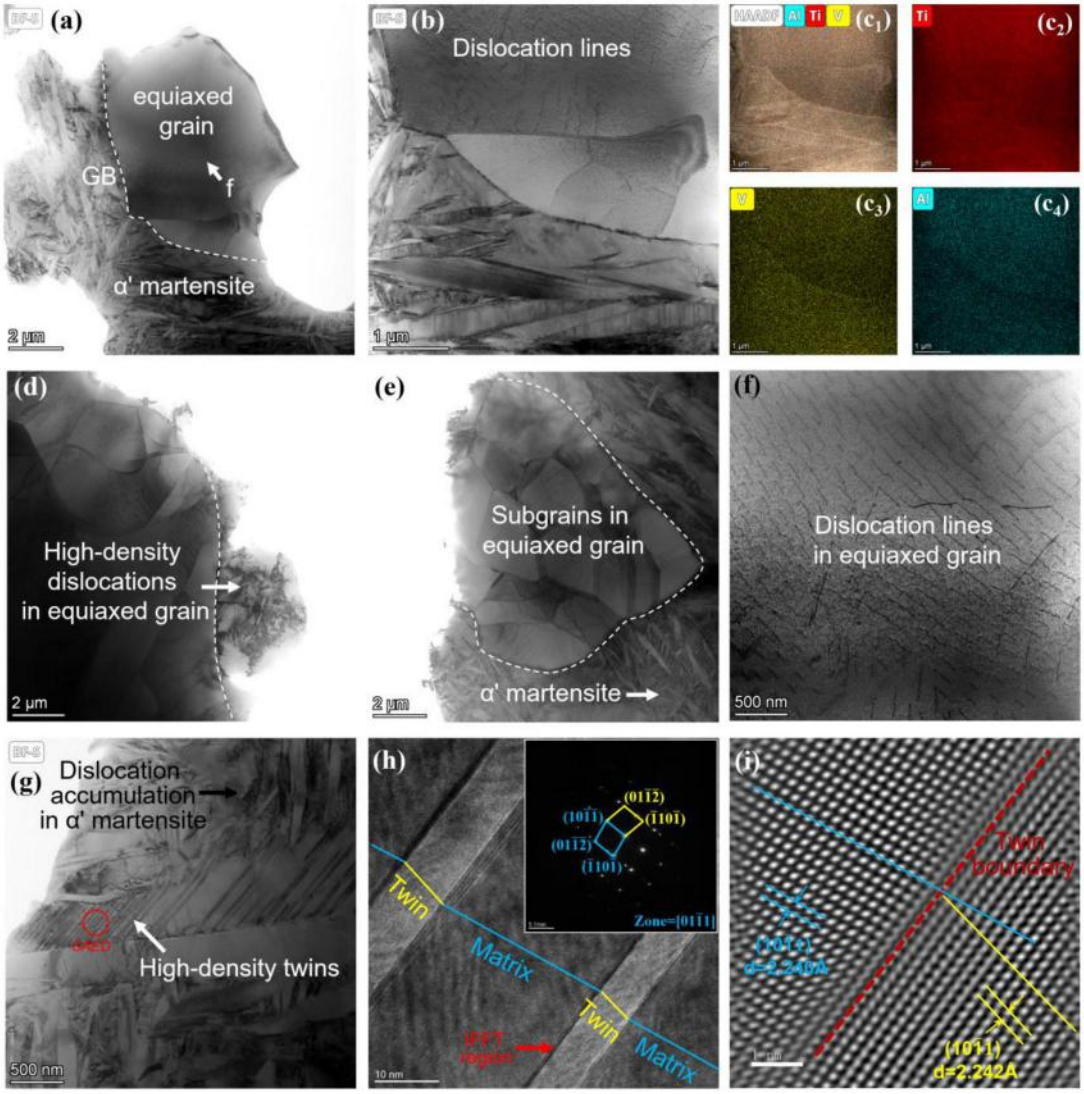


Figure 6. TEM microstructures of the WQ alloy. (a), (b) BF-S images. (c_1) High-angle annular dark-field (HAADF) image together with the EDS image for Ti, V, and Al. (c_2–c_4) EDS images showing the elemental distribution of Ti, V, and Al, respectively. (d), (e) BF-S images showing the microstructure of the large equiaxed grains. (f) Magnified image of the marked region in (a). (g) BF-S images showing the twins in acicular α' martensite. (h) HRTEM image of the twinned region in (g), the inset shows the SAED pattern of the marked region in (g). (i) IFFT image of the marked region in (h).

different deformation behaviors among different α grains during hot forging. It is known that the lamellar grain is easier to deform than the equiaxed grain during hot forging. Therefore, the dislocation accumulation is not significant in the equiaxed grains and only a few high-density regions can be observed. On the other hand, the acicular α′ martensite grains not only show high dislocation density, but also high-density twins (Fig. 6g–i). Such twins are confirmed to be $(10\bar{1}\bar{1})$ transformation twins, which have been widely reported to appear in titanium alloys after water quenching process [28, 29].

The WQ alloy exhibits unique microstructural features, in which the high strength is mainly attributed to the existence of α′ martensite. First, the high dislocation density in α′ martensite will lead to the strengthening effect owing to the difficult dislocation motion [30, 31]. Second, the nanosized acicular α′ martensite grains with interior high-density twins can provide large amounts of grain boundaries and twin boundaries. These boundaries can hinder the dislocation motion and therefore strengthen the alloys [32]. Although the WQ alloy was strengthened by nanosized α′ martensite, the ductility decreases at the same time. This is reasonable because the difficult dislocation motion is not beneficial to the large deformability and elongation.

4.2 Origin of strength–ductility synergy of the ST alloy

It was discussed that the acicular martensite in the WQ alloy can enhance the tensile strength but decrease the ductility. Notably, the ST alloy shows an increased elongation and maintains a similar tensile strength compared to the WQ alloy, implying the low temperature short time annealing can improve the ductility without sacrificing the strength. This is also attributed to the microstructure features of the ST alloy.

Figure 7a shows the TEM microstructure of the ST alloy. It can be observed that the large equiaxed grain and fine acicular α′ martensite coexist in the alloy. Although the grain size and morphology of ST alloy are similar to that of the WQ alloy, the dislocation features in these alloys are quite different. As displayed in Fig. 7a and b, the dislocation density is low, and few dislocation lines can be

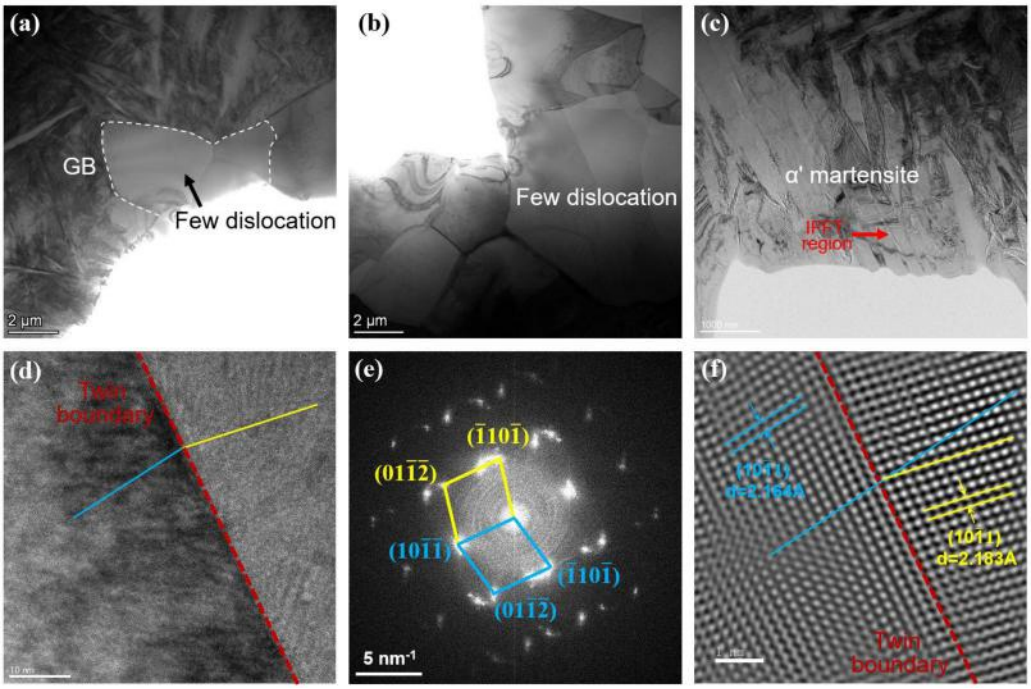


Figure 7. TEM microstructures of the ST alloy. (a–c) BF-S images. (d) HRTEM image of the twinned region in (c). (e) FFT diffraction pattern of the region shown in (d). (f) IFFT image of the twin boundary region shown in (d).

observed in the equiaxed grains. Such dislocation features in large equiaxed grains are attributed to the dislocation annihilation during annealing process. However, the annealing temperature and time in this work is not high and long enough to lead to a complete recovery in both equiaxed grains and acicular martensite grains. Therefore, the dislocation density is still quite high in the acicular martensite grains after annealing (Fig. 7c). Besides, the transformation twins still exit within the martensite grains as displayed in Fig. 7d–f. Consequently, for the ST alloy, the acicular α′ martensite grains with high dislocation density and large amounts of twins strengthen the alloy and contribute to the high tensile strength, which is similar to the strengthening mechanism in the WQ alloy. Importantly, compared to the fine acicular grains, the large equiaxed grains with few dislocations can enhance the work hardening ability of the alloy and improve the ductility [33]. Thus, the heterogeneous dual-phase α + α′ structure can cause a superior strength–ductility synergy owing to its unique dislocation distribution and features. The dense nanosized acicular martensite contributed to the high strength, and the dislocation-free large equiaxed grains contributed to the high ductility.

In summary, we proposed a specialized thermal-mechanical processing method for Ti-6Al-4V alloy, which is promising to be used in the industrial manufacturing process of high-performance Ti-6Al-4V as well as other titanium alloys. In order to further improve the mechanical properties, future studies may focus on the effect of processing parameters (e.g. forging temperature, strain rate, cooling rate) on the microstructure evolution of titanium alloy.

5. Conclusion

In the present work, the strength–ductility balance was achieved in Ti-6Al-4V alloy through specialized hot forging and short time annealing processes. The microstructure evolution and the origin of superior mechanical properties have been investigated in detail. The conclusions are summarized as follows:

(1) The FG alloy shows the microstructure composed of large and fine globular α grains. The large equiaxed grains were inherited from the bimodal as-received alloy, which barely changed during hot forging process. The fine globular α grains were formed due to the dynamic recrystallization of lamellar α grains during hot forging. Consequently, the heterogeneous fine/large equiaxed structure was obtained after hot forging process.

(2) The WQ alloy shows the microstructure composed of large equiaxed grains and nanosized acicular α′ martensite grains. Such microstructure formed because the large equiaxed grains nearly remained unchanged during water quenching, whereas the martensite transformation occurred within fine equiaxed grains during water quenching. Compared to the FG alloy, the WQ alloy exhibits a significantly increased tensile strength and a decreased elongation. The strengthening effect came from the high dislocation density, high-density grain boundaries, and dense twin boundaries in the region of α′ martensite.

(3) The ST alloy shows the similar grain size and grain morphology to the WQ alloy, including the large equiaxed grains and nanosized acicular α′ martensite grains. Similarly, the dislocation density is high in the acicular α′ martensite grains and the nano twins still remained within the grains. However, the dislocation density in large equiaxed grains dramatically decreased after short time annealing. Consequently, the ST alloy shows an increased elongation and maintains a similar tensile strength compared to the WQ alloy, implying the low temperature short time annealing can improve the ductility without sacrificing the strength.

Author contributions

Shenshi Jiang (Writing—original draft, Validation, Data curation, Formal analysis), Guangqing Zhang (Methodology, Project

administration, Resources, Supervision), Lisong Zhu (Data curation, Investigation, Formal analysis), Qian Wang (Data curation, Investigation), Feijun Qu (Methodology, Validation, Supervision), Jun Wang (Investigation), Yao Lu (Investigation), and Jian Han (Conceptualization, Methodology, Project administration, Supervision, Validation, Writing—review & editing).

Conflict of interest

None declared.

Funding

None declared.

Data availability

The data underlying this article will be shared on reasonable request to the corresponding author.

References

[1] Banerjee D, Williams JC. Perspectives on titanium science and technology. *Acta Mater* 2013;**61**:844–79. https://doi.org/10.1016/j.actamat.2012.10.043

[2] Najafizadeh M, Yazdi S, Bozorg M *et al.* Classification and applications of titanium and its alloys: a review. *J Alloy Compd Commun* 2024;**3**:100019. https://doi.org/10.1016/j.jacomc.2024.100019

[3] Zhao Q, Sun Q, Xin S *et al.* High-strength titanium alloys for aerospace engineering applications: a review on melting-forging process. *Mater Sci Eng A* 2022;**845**:143260. https://doi.org/10.1016/j.msea.2022.143260

[4] Wen X, Wan M, Huang C *et al.* Strength and fracture toughness of TC21 alloy with multi-level lamellar microstructure. *Mater Sci Eng A* 2019;**740-741**:121–9. https://doi.org/10.1016/j.msea.2018.10.056

[5] Zhang CL, Bao XY, Zhang DD *et al.* Achieving superior strength–ductility balance in a novel heterostructured strong metastable β-Ti alloy. *Int J Plast* 2021;**147**:103126. https://doi.org/10.1016/j.ijplas.2021.103126

[6] Zhang YS, Hu JJ, Zhang W *et al.* Discontinuous core-shell structured Ti-25Nb-3Mo-3Zr-2Sn alloy with high strength and good plasticity. *Mater Charact* 2019;**147**:127–30. https://doi.org/10.1016/J.MATCHAR.2018.10.021

[7] Mantri SA, Choudhuri D, Alam T *et al.* Tuning the scale of α precipitates in β-titanium alloys for achieving high strength. *Scr Mater* 2018;**154**:139–44. https://doi.org/10.1016/j.scriptamat.2018.05.040

[8] Bao X, Chen W, Zhang J *et al.* Achieving high strength–ductility synergy in a hierarchical structured metastable β-titanium alloy using through-transus forging. *J Mater Res Technol* 2021;**11**:1622–36. https://doi.org/10.1016/j.jmrt.2021.02.012

[9] Hua K, Zhang Y, Tong Y *et al.* Enhanced mechanical properties of a metastable β titanium alloy via optimized thermomechanical processing. *Mater Sci Eng A* 2022;**840**:142997. https://doi.org/10.1016/j.msea.2022.142997

[10] Dumas O, Malet L, Kwaśniak P *et al.* Reorientation induced plasticity (RIP) in high-strength titanium alloys: an insight into the underlying mechanisms and resulting mechanical properties. *Acta Mater* 2023;**246**:118679. https://doi.org/10.1016/j.actamat.2023.118679

[11] Ouyang W, Zhang L, Wu H *et al.* Optimized mechanical properties of the hot forged Ti–6Al–4V alloy by regulating multiscale microstructure via laser shock peening. *Int J Mach Tools Manuf* 2024;**201**:104192. https://doi.org/10.1016/j.ijmachtools.2024.104192

[12] Lett S, Cormier J, Quet A *et al.* Microstructure optimization of cold sprayed Ti-6Al-4V using post-process heat treatment for improved mechanical properties. *Addit Manuf* 2024;**86**:104168. https://doi.org/10.1016/j.addma.2024.104168

[13] Shen J, Zhang Z, Xie J. Annealing microstructure evolution and strength–plasticity enhancement mechanism of a novel titanium alloy Ti6422. *Mater Sci Eng A* 2024;**897**:146338. https://doi.org/10.1016/j.msea.2024.146338

[14] Xu M, Xiao L, Gao B *et al.* Strengthening mechanisms induced by sequential grain refinement and solid solution strengthening in dual-phase heterostructured Mg-Li alloys with low Al content. *J Alloys Compd* 2025;**1021**:179527. https://doi.org/10.1016/j.jallcom.2025.179527

[15] Nie J, Chen Y, Song L *et al.* Enhancing strength and ductility of Al-matrix composite via a dual-heterostructure strategy. *Int J Plast* 2023;**171**:103825. https://doi.org/10.1016/j.ijplas.2023.103825

[16] Fang XT, He GZ, Zheng C *et al.* Effect of heterostructure and hetero-deformation induced hardening on the strength and ductility of brass. *Acta Mater* 2020;**186**:644–55. https://doi.org/10.1016/j.actamat.2020.01.037

[17] Cao L, Zhang Y, Gao H *et al.* Heterostructure-induced anisotropy of tensile property in laser directed energy deposition TC11 titanium alloy. *Mater Sci Eng A* 2024;**916**:147349. https://doi.org/10.1016/j.msea.2024.147349

[18] Zhu Y, Wu X. Heterostructured materials. *Prog Mater Sci* 2023;**131**:101019. https://doi.org/10.1016/j.pmatsci.2022.101019

[19] Lin T, Zhou L, Guo Y *et al.* Synergic strength–ductility enhancement in bimodal titanium alloy via a heterogeneous structure induced by the ⟨c + a⟩ slip. *J Mater Sci Technol* 2025;**204**:255–67. https://doi.org/10.1016/j.jmst.2024.04.012

[20] Jia Y, Su H, Cao S *et al.* Fabrication of highly heterogeneous precipitate microstructure in an α/β titanium alloy. *Acta Mater* 2024;**279**:120302. https://doi.org/10.1016/j.actamat.2024.120302

[21] Meng L, Zhao Z, Lin P *et al.* Achieving enhanced strength–ductility synergy in heterogeneous equiaxed structured Ti-6Al-4V alloy sheets by cryogenic pre-stretching. *Mater Des* 2025;**249**:113563. https://doi.org/10.1016/j.matdes.2024.113563

[22] Yang H, Zhu M, Chen N *et al.* Novel hierarchical α structure enhanced strength–ductility synergy in metastable β titanium alloy. *Mater Sci Eng A* 2025;**925**:147877. https://doi.org/10.1016/j.msea.2025.147877

[23] Feng T, Luo Z, Ma X. A strategy for simultaneously enhancing the strength and ductility of metastable β titanium alloys: coupling heterogeneous structure and TRIP effects. *Mater Sci Eng A* 2024;**915**:147264. https://doi.org/10.1016/j.msea.2024.147264

[24] Dai J, Tang B, Wang C *et al.* Simultaneously achieving exceptional and heat treatment insensitive strength–ductility synergy in an α+β titanium alloy via tailoring silicide and heterogeneous α precipitates. *J Mater Sci Technol* 2025;**236**:51–66. https://doi.org/10.1016/j.jmst.2025.01.072

[25] Yu H, Li W, Li S *et al.* Study on transformation mechanism and kinetics of α' martensite in TC4 alloy isothermal aging process. *Crystals (Basel)* 2020;**10**:229. https://doi.org/10.3390/cryst10030229

[26] Boccardo AD, Zou Z, Simonelli M *et al.* Martensite decomposition kinetics in additively manufactured Ti-6Al-4V alloy: in-situ characterisation and phase-field modelling. *Mater Des* 2024;**241**:112949. https://doi.org/10.1016/j.matdes.2024.112949

[27] Qazi JI, Senkov ON, Rahim J *et al.* Kinetics of martensite decomposition in Ti-6Al-4V-xH alloys. *Mater Sci Eng A* 2003;**359**:137–49. https://doi.org/10.1016/S0921-5093(03)00350-2

[28] Li K, Yang J, Yi Y *et al.* Enhanced strength–ductility synergy and mechanisms of heterostructured Ti6Al4V-Cu alloys produced by laser powder bed fusion. *Acta Mater* 2023;**256**:119112. https://doi.org/10.1016/j.actamat.2023.119112

[29] Cao S, Zhang B, Yang Y *et al.* On the role of cooling rate and temperature in forming twinned α' martensite in Ti–6Al–4V. *J Alloys Compd* 2020;**813**:152247. https://doi.org/10.1016/j.jallcom.2019.152247

[30] Zhang C, Zhang J, Bao X *et al.* Hierarchically ordered coherent interfaces-driven ultrahigh specific-strength and toughness in a nano-martensite titanium alloy. *Acta Mater* 2024;**263**:119540. https://doi.org/10.1016/j.actamat.2023.119540

[31] Xin T, Zhao Y, Mahjoub R *et al.* Ultrahigh specific strength in a magnesium alloy strengthened by spinodal decomposition. *Sci Adv* 2021;**7**:eabf3039. https://doi.org/10.1126/sciadv.abf3039

[32] Cheng Z, Bu L, Zhang Y *et al.* Unraveling the origin of extra strengthening in gradient nanotwinned metals. *Proc Natl Acad Sci USA* 2022;**119**:e2116808119. https://doi.org/10.1073/pnas.2116808119

[33] Yang M, Pan Y, Yuan F *et al.* Back stress strengthening and strain hardening in gradient structure. *Mater Res Lett* 2016;**4**:145–51. https://doi.org/10.1080/21663831.2016.1153004

© The Author(s) 2025. Published by Oxford University Press on behalf of Taiyuan University of Technology.
This is an Open Access article distributed under the terms of the Creative Commons Attribution License (https://creativecommons.org/licenses/by/4.0/), which permits unrestricted reuse, distribution, and reproduction in any medium, provided the original work is properly cited.
Composite Design and Manufacturing, 2025, 1, 69–76
https://doi.org/10.1093/cdm/wqaf007
Research Article



https://dspace.org/

Towards strength–ductility balance in a Ti-6Al-4V alloy through microstructure optimization by composite hot forging and two-step annealing processes

Jiang, Shenshi; Zhang, Guangqing; Zhu, Lisong; Wang, Qian; Qu, Feijun ...

2025-10-01
Oxford University Press (OUP)
https://doi.org/10.1093/cdm/wqaf007
Jiang S, Zhang G, Zhu L, et al., (2025) Towards strength–ductility balance in a Ti-6Al-4V alloy through microstructure optimization by composite hot forging and two-step annealing processes. Composite Design and Manufacturing, Volume 1, Issue 2, October 2025, Article number wqaf007

Downloaded from a DSpace repository. https://dspace.org/